Dual TBX5-Lineage and MYL2 Reporter System For Identification of Left Ventricular Cardiomyocytes During Human Induced Pluripotent Stem Cell Differentiation

Francisco X. Galdos[1,2], BA, Carissa Lee[1], Soah Lee, PhD[1,2], William Goodyer, MD, PhD[1,3], Sharon Paige, MD, PhD[1,3], Sidra Xu[1], Gabriela V. Escobar[1], Rasmus O. Bak, PhD[6], Matthew Porteus, MD, PhD[1,5], Sean M. Wu, MD, PhD[1,2,4]

[1]Stanford Cardiovascular Institute, [2] Institute for Stem Cell Biology and Regenerative Medicine, Stanford University, [3]Division of Pediatric Cardiology, Department of Pediatrics [4] Division of Cardiovascular of Medicine, Department of Medicine, [5]Department of Pediatrics, Stanford University School of Medicine, Stanford CA
[6]Department of Biomedicine, Aarhus University, Aarhus, Denmark

*Correspondance:
Sean M. Wu, MD, PhD
G1120 Lokey Stem Cell Building
265 Campus Drive
Stanford, CA 94305
smwu@stanford.edu

Keywords
Cardiac Development, transcription factor, cardiomyocyte differentiation, pluripotent stem cells, lineage tracing, genetic engineering

ABSTRACT

Rationale: Patient-derived induced pluripotent stem cells (iPSCs) present an exciting avenue for the modeling congenital heart disease. While hiPSC cardiac differentiations generate various cell types, the presence of mixed cell populations can confound interpretation of study results, particularly in the case of modeling structural congenital heart defects where lesions affect specific chambers of the heart. During cardiac development, the left and the right ventricles arise from distinct cardiac progenitor populations known as the first and second heart fields, respectively. Currently, availability of a lineage tracing tool to identify the descendants of these progenitors in the human iPSC system is lacking and such a tool would allow for the identification of left and right ventricular cardiomyocytes for modeling of chamber specific congenital heart defects *in vitro*.

Objectives: Genetically engineer a heart field-specific lineage tracing and a ventricular specific genetic reporter system in human iPSCs to identify left and right ventricular cardiomyocytes *in vitro.*

Methods and Results: We gene targeted a TBX5-based Cre-LoxP lineage tracing system via CRISPR/Cas9 genome editing into an hiPSC line from a healthy male patient. We also replaced the stop codon of the ventricular-specific Myosin Light Chain-2 (MYL2) gene with a P2A-TdTomato construct to allow for the identification of ventricular cardiomyocytes through the course of differentiation. Using a standard small molecular biphasic WNT modulation protocol, we conducted multiple independent differentiations and analyzed by FACS the percentage of lineage positive and troponin-T (TNNT2+) positive cardiomyocytes at multiple timepoints during differentiation. Analysis of GFP+ (TBX5-lineage+) cells out of TNNT2+ cells identified a gradual increase in GFP expression beginning at day 11 of differentiation and results in nearly 100% of TNNT2+ cardiomyocytes exhibiting GFP expression. GFP+ expression among MYL2-Tomato+ cells confirmed the predominance of TBX5-lineage+ ventricular cardiomyocytes. Analysis of gene expression across differentiation confirmed the predominance of LV marker genes and the absence or downregulation of SHF and RV markers.

Conclusions: Here, we genetically engineered a triple-targeted dual-fluorescent hiPSC reporter line that allows for the identification of TBX5-lineage positive ventricular cardiomyocytes. Gene expression analysis confirms the predominance of a left ventricular phenotype consistent with the fluorescence reporter expression. In summary, we provide a powerful tool for identifying and isolating chamber-specific left ventricular cardiomyocytes.

INTRODUCTION

Congenital heart defects affect approximately 40,000 births per year in the United States alone, with 1 in 4 children with CHD presenting with life-threatening defects (Reller et al., 2008). While genetic wide association studies have aimed to identify the genetic etiologies of multiple types of CHD, the etiology of these complex defects remains poorly understood (Lahm et al., 2021). Importantly, the human heart is one of the first organs to develop during embryogenesis with critical events in cardiogenesis being completed by around 5 weeks of human gestation (Asp et al., 2019; Buijtendijk et al., 2020; Cui et al., 2019). Due to ethical and technical limitations in the study of human embryogenesis prior to 5 weeks of gestation, developmental biologists have largely relied on animal models to study cardiac development (Cavaliere, 2017). Over the past decade, the advent of human pluripotent stem cell technology has unlocked the potential to study the development of multiple organ systems using an *in vitro* setting (Chen et al., 2016; Rowe and Daley, 2019). In the cardiac field, highly successful small molecule protocols allow for the generation of beating cardiomyocytes that have been utilized for disease modeling, drug discovery, and the study of cellular functions (Chen et al., 2016; Feyen et al., 2020; Lian et al., 2013; Sacchetto et al., 2020). Importantly, hiPSCs can be derived from patients exhibiting a particular disease of interest which has allowed for the disease modeling of multiple cardiac illnesses including congenital heart defects (Hrstka et al., 2017; Miao et al., 2020; Paige et al., 2020; Rhee et al., 2021; Yang et al., 2017).

While hiPSCs have provided a powerful tool for disease modeling and the study of cardiac development *in vitro*, data is lacking on the types of cardiomyocytes that are being generating during cardiac differentiation. The mammalian heart is derived from two populations of cardiac progenitors known as the first (FHF) and second (SHF) heart fields (Meilhac et al., 2004; Meilhac and Buckingham, 2018; Rana et al., 2014; Zaffran et al., 2004). The FHF is the first population of progenitor cells that arises from the mesoderm germ layer during gastrulation and gives rise to the left ventricle (LV) and parts of the atria (Bruneau et al., 2001, 1999; Devine et al., n.d.; Meilhac et al., 2004). The second heart field contributes to the development of the right ventricle (RV), atria, and the outflow tract (Cai et al., 2003; Meilhac and Buckingham, 2018; Rana et al., 2014; Zaffran et al., 2004). Interestingly, specific CHDs such as single ventricle diseases where specific chambers are underdeveloped or atretic raise questions of whether defects within specific cardiomyocyte populations contribute to these diseases. While efforts have been conducted to differentiate hiPSCs into specific cardiomyocyte populations such as atrial, ventricular, and pacemaker-like cell types (Lee et al., 2017; Protze et al., 2017), little is understood on whether current hiPSC differentiation protocols give rise to FHF- and SHF-derived LV and RV cardiomyocytes, respectively.

In the murine system, multiple studies have identified specific gene markers for identifying FHF and SHF progenitors. Early studies profiling the expression of the T-box transcription factor, *Tbx5,* identified its specific expression at the cardiac crescent which represents the early FHF progenitors of the heart (Bruneau et al., 2001, 1999). Importantly, *in situ* hybridization experiments have identified the highly specific expression of *Tbx5* in the atria and left ventricle in E7.75-E11.5 mouse hearts (Bruneau

et al., 1999). More recently, studies using an inducible CreER/LoxP lineage tracing mouse line have shown the exquisite specificity of *Tbx5* to label left ventricular cells and demonstrate a clear boundary between the LV and RV during embryogenesis that is marked by this lineage tracing reporter line (Devine et al., 2014). Lastly, scRNA-seq studies have further confirmed the specificity of *Tbx5* as a FHF and LV marker suggesting its high specificity for identifying LV vs RV cardiomyocytes (Cui et al., 2019; de Soysa et al., 2019; DeLaughter et al., 2016; Li et al., 2016).

Currently, no lineage tracing system exists in the hiPSC system that would allow for the tracing of LV and RV cardiomyocytes in a human system. Identifying these two subtypes of cardiomyocytes is critical to modeling chamber specific congenital heart defects and to gain a greater understanding of the transcriptional pathways the regulate the development of these two chambers. Here, we targeted a highly sensitive TBX5 driven Cre/LoxP lineage tracing system into hiPSCs containing a ventricular-specific myosin light chain-2 (*MYL2)* driven TdTomato fluorescent protein. By conducting a time course analysis of cardiomyocyte differentiation, we identified a left ventricular predominant differentiation based on the high percentage of TBX5-lineage positive cardiomyocytes and validated the high expression of LV-specific markers.

METHODS

Cell Lines:

Human induced pluripotent stem cell line used in this study was provided by the Stanford Cardiovascular Institute Biobank (SCVI-111, Sendai virus reprogrammed peripheral blood mononuclear cells, healthy male with normal karyotype, 46, XY).

Cardiac Differentiation:

HiPSCs were maintained in DMEM/F12 (ThermoFisher) supplemented with essential eight (E8) (henceforth referred to as E8 media) that is prepared in-house as previously described (Burridge et al., 2015) and cultured on growth factor reduced Matrigel (Corning) coated plates at a 1:350 dilution. Upon reaching 75-80% confluency, hiPSCs were passaged using 0.5 mM EDTA in PBS for 8 minutes at 37°C. Passaging was conducted with gentile dissociation of cell clusters and plated in E8 media supplemented 10μM ROCK inhibitor. Passaging was performed using 1:12 splitting ratio to achieve approximately 10,000 cells per cm^2. 24 hours after passaging media was changed to E8 media. Daily media changes were conducted until cells reached 90-95% confluency at which point media was change to RPMI-1640 containing 6μM CHIR99021 (Selleckchem) and 2% B27 minus insulin supplement (Invitrogen). Two days after initial treatment with CHIR, media was changed to RPMI-1640 with 2% B27 minus insulin for 24 hrs. Between day 3-5, media was changed to 2μM C59 in RPMI-1640 media with 2% B27 minus insulin. On day5 of differentiation, media was changed for RPMI-1640 with 2% B27 minus insulin for 48 hrs and was subsequently changed to RPMI-1640 with 2% B27 Plus Insulin for another 48 hrs. On day 9, cells underwent glucose deprivation for 48 hrs to purify cardiomyocytes by changing media to RPMI-1640 minus glucose with 2% B27 Plus insulin. Cardiomyocytes were subsequently maintained in RPMI-1640 with glucose with 2% B27 Plus Insulin.

Donor Construct Plasmid Constructs

Cre recombinase gene sequence was provided by Connie Cepko lab (Addgene plasmid # 13775) (Matsuda and Cepko, 2007). TurboGFP gene was obtained from the pMaxGFP plasmid obtained from the Lonza P3 Primary Cell 4D-Nucleofector X Kit L. Plasmids were constructed using plasmid construct service by GenScript Biotech.

CRISPR/Cas9 Genome Editing:

Genetic constructs were targeted to hiPSCs following the schematic presented in Figure 1. TurboGFP sequence was obtained from Protocol for targeting of genetic constructs was followed as previously described (Galdos et al., 2021). Briefly, hiPSCs were dissociated into a single cell suspension at 75% confluency using an Accutase-EDTA solution (Millipore) containing a 0.02% blebbistatin (Sigma-Aldrich). Dissociation reaction was quenched using a solution of E8 media with 10μM ROCK inhibitor an 0.02% blebbistatin. Cells were then pelleted by centrifugation at 200g for 3 minutes. We subsequently conducted nucleofection of the dissociated cells using the Lonza P3 Primary Cell 4D-Nucleofector X Kit L. A transfection mix was prepared containing the Lonza P3 Solution, Supplement, single guide RNA/Cas9 expressing plasmid (1μg), and the donor template plasmid (3μg). Cells were electroporated using a Lonza 4D Nucleofector machine using protocol number “CM150”. After electroporation, 1 mL of E8 media supplemented with 10μM ROCK inhibitor was gently added to the cuvette containing the cells. Cells were allowed to rest for 10 minutes after which they were plated onto two wells of a 6 well plate. 24 hrs after plating, media was changed to regular E8 media, and regular maintenance until cells reach 50% confluency. At the 50% confluency mark, cells were dissociated into single cell suspensions and passaged

onto 6 well plates at 1000 cells per well of 6-well. We subsequently maintained the transfected hiPSCs in E8 media supplemented with appropriate antibiotic for selection of successfully targeted cells. Concentrations were as follows for the constructs targeted: TBX5-Cre (Hygromycin 150 µg/mL), CCR5-CLSL-TurboGFP (G418 150 µg/mL), and MYL2-Tdtomato (Puromycin 0.2 µg/mL). After 5 days of treatment with antibiotic, cells were switched to regular E8 to allow for colony expansion derived from single cells plated. After 4 days of colony expansion, colonies were picked into 24-well plates containing E8 plus 10 µM ROCK inhibitor and were expanded for downstream DNA extraction using Qiagen DNeasy Kit and for cell freezing using Bambanker.

PCR validation of construct integration was conducted using the “Inside-Outside” approach where one primer was designed outside of the homology arms of the donor template and one primer was designed insight of the construct to be integrated. PCRs were conducted using the GoTaq Master Mix (Promega Corporation), and products were run on a 1% agarose gel in 1X TAE Buffer.

Flow Cytometry:

A Beckman Coulter CytoFLEX flow cytometer was used for high throughput analysis of TNNT2, TurboGFP, and TdTomato expression across time of hiPSC cardiac differentiation. On day of timepoint collection, cells were dissociated into single cell suspensions by incubating in 10X TrypLE Select (ThermoFisher) for 5 minutes at 37 degrees Celsius. For later stage cardiomyocytes (day 15 and onwards) incubation time was extended to 10 minutes to achieve single cell dissociation. Cells were subsequently pelleted by centrifugation at 200g for 5 minutes. Cell pellets were resuspended in 4% PFA for 10 minutes and were rinsed with a 5% Fetal Bovine Serum solution in 1x PBS.

Cells were permeabilized in a 0.5% Saponin solution containing 5% FBS in 1X PBS (hereafter refered to as Saponin Solution). After permeabilization cells were incubated for 45 minutes in a monoclonal mouse anti-Troponin primary antibody (ThermoFisher Cat**.** MA5-12960) at a 1:200 dilution in 0.5% saponin solution. Cells were rinsed twice in saponin solution and then incubated in secondary antibody AlexaFluor 647 goat anti-mouse (ThermoFisher) at a 1:1000 dilution in 0.5% saponin solution. Cells were subsequently rinsed in 1x PBS twice and analyzed using CytoFLEX flow cytometer.

RNA Extraction and Quantitative RT-PCR

Cells were collected for RNA extraction by dissociation with 10X TrypLE Select and pelleted as described in the Flow Cytometry section. Cell pellets were then resuspended in 300 µL of TRIZOL reagent (Invitrogen) at room temperature for 3 minutes. After complete resuspension of the cells, RNA was extracted using the Zymo DIRECT-Zol extraction kit per manufacuter's protocol. Purified RNA was reverse transcribed into cDNA using the High-Capacity RNA-to-cDNA kit (ThermoFisher). Quantitative PCR was subsequently run on a Biorad qPCR 384-well machine using the Biorad SYBR qPCR master mix.

Statistics:

Data are presented as a mean ± standard error of the mean. Minimum of four independent biological replicates were used for all experiments (i.e. independent cardiac differentiations were collected for all experiments).

RESULTS

CRISPR-Cas9-mediated gene targeting to generate TBX5-Lineage Tracing and Ventricular Reporter Line

To generate a fluorescent reporter system that would allow us to lineage trace left ventricular cardiomyocytes during hiPSC differentiation, we designed a triple construct system that would allow for the identification of *MYL2*-positive ventricular cardiomyocytes and the *TBX5*-lineage FHF lineage cells, including left ventricular cardiomyocytes. Our strategy allows for the identification of left ventricular cardiomyocytes that are TBX5-lineage+/MYL2+ and right ventricular cardiomyocytes that are TBX5-lineage-/MYL2+ (**Figure 1A**). We have previously published the use of an *MYL2*-TdTomato construct targeting a P2A-TdTomato to the stop codon of the *MYL2* gene that was validated to specifically isolate ventricular cardiomyocytes during hiPSC differentiations (Chirikian et al., 2021). The P2A self-cleaving peptide allows for the tethering of the TdTomato expression to the *MYL2* gene while minimizing disruptions to the endogenous *MYL2* protein (Liu et al., 2017) (**Figure 1B**). To lineage trace *TBX5* expressing cells during hiPSC differentiation, we targeted a highly sensitive reporter construct consisting of two tandem P2A-Cre Recombinase constructs to replace the stop codon of the *TBX5* gene. We subsequently targeted a CMV driven TurboGFP with a floxed stop cassette to the *CCR5* safe harbor locus such that TurboGFP expression could only occur after the excision of the stop cassette by Cre recombinase (**Figure 1B**). To confirm successful integration of the genetic constructs into an hiPSC line, we conducted a sequential integration approach where we first integrated the *MYL2*-TdTomato construct, followed by the CCR5 construct, and lastly by integration of the TBX5-Cre construct. We confirmed the integration of all three constructs in a single

hiPSC line by conducting inside-outside PCR. For both the MYL2 and CCR5 constructs we selected clones displaying a heterozygous integration pattern, while a homozygous integration pattern was selected for the TBX5-Cre construct to maximize sensitivity of TBX5 lineage tracing (**Figure 1C**). We further confirmed the in-frame integration of the reporter Tdtomato and Cre Recombinase into the *MYL2* and *TBX5* loci, respectively, by sanger sequencing (**Figure 1D**). Together, these results demonstrated the successful genome editing of a triple construct into a single hiPSC line.

Cardiomyocyte Differentiation of TBX5-Lineage/MYL2 Reporter Line Reveal Predominance of Left Ventricular Cardiomyocytes

To determine the proportion of hiPSC-derived cardiomyocytes that exhibit a TBX5-lineage positive phenotype, we conducted cardiac differentiations using a standard biphasic WNT protocol (**Figure 1A**) and conducted a time course flow cytometry analysis of the percentage of TurboGFP+ (representing TBX5-lineage-positive) out of all cardiomyocytes during differentiation and within the definitive ventricular myocyte population. To evaluate the percentage of cardiomyocytes during differentiation we conducted cardiac troponin T (TNNT2) staining and evaluated the expression of TurboGFP across differentiation (**Figure 2B**). We observed the gradual increase in TNNT2 expression starting at Day 7 of differentiation with the expression of TurboGFP initiating by Day 11. The percentage of TurboGFP+ cardiomyocytes gradually increased through differentiation reaching a mean of 95.6% ± 0.94% across 8 independent differentiations (**Figure 2B and 2C**). To evaluate the percentage of definitive ventricular cardiomyocyte that express TurboGFP, we analyzed the

percentage of totals cells during differentiation that expressed the TdTomato fluorescent protein through differentiation. As expected, *MYL2* expression gradually increased over time consistent with the known upregulation of *MYL2* through the course of ventricular maturation previously observed (**Figure 2D**). Interestingly, regardless of timepoint analyzed, the percentages of TurboGFP+ cells out of TdTomato+ cells were >95% indicating the predominance of TBX5-lineage positive cardiomyocytes (**Figures 2E, 2F, 2G**).

To determine whether the high GFP percentages were indicative of a left ventricular phenotype, we conducted gene expression analyses across multiple timepoints during hiPSC differentiation for known markers of left and right ventricular development. We evaluated the expression of *HAND1*, a specific marker distinguishing the early FHF and LV (Barnes et al., 2010; de Soysa et al., 2019), *TBX5,* and Cre Recombinase expression (**Figure 3A)***.* As expected, we observed a gradual upregulation of TBX5 and Cre Recombinase and high expression of *HAND1* across multiple timepoints of development. Relative to day 0 we observed that all three markers exhibited high expression values with *Hand1* exhibiting more than 50,000 fold upregulation relative to day 0 by day 7 of differentiation. Moreover, by day 30 of development *TBX5* exhibited nearly 3000-fold upregulation indicating a high overall expression in the hiPSC cardiomyocytes.

Analysis of second heart field markers,*TBX1* and *FGF8* (Park et al., 2008; Rana et al., 2014)*,* revealed a small upregulation with approximately 2.2-fold upregulation during day 3-7 of differentiation with a sharp decrease after the day 7 timepoint (**Figure 3B**). By day 20, anterior SHF markers *TBX1* and *FGF8* exhibited a marked

downregulation relative to day 0. None of these markers exhibited the dramatic upregulation seen from *HAND1* and *TBX5.* We also analyzed the expression of *ISL1* which has been previously reported as second heart field marker (Cai et al., 2003), however, more recently it has been well known to be expressed in both heart field progenitors (Ma et al., 2008). As expected, we observed a sharp upregulation at day 5, consistent with the cardiac progenitor stage, and gradual downregulation through the course of differentiation. Lastly, we also observed a gradual upregulation of cardiomyocyte markers as well as known ventricular cardiomyocyte marker *MYL3* and *MYL2* consistent with our flow cytometry data showing gradual increase of *MYL2-TdTomato* expression through differentiation.

DISCUSSION

In this paper, we describe the generation of a triple-targeted dual fluorescent reporter system that allows for lineage tracing *TBX5* expressing cells through the course of hiPSC differentiation. As previously reported, *TBX5* is one of the first markers to have been reported as a specific marker for the FHF and has been shown to exhibit exquisite specificity to the left ventricle during early stages of murine embryonic development. Here, we successfully implemented a *TBX5* lineage tracing scheme into the hiPSC system designing by a highly sensitive Cre recombinase targeting construct that was integrated into two alleles of *TBX5*. Moreover, by including an *MYL2*-TdTomato direct reporter into our hiPSC line, we evaluated the percentage of ventricular cardiomyocytes that descended from *TBX5* expressing precursors. Unexpectedly, our data indicates that within the hiPSC line analyzed the predominant phenotype observed is a TBX5-

lineage-positive cell across more than 95% of all cardiomyocytes generated. Gene expression analysis also revealed the high expression levels of FHF markers *HAND1* and *TBX5* with significantly lower expression of SHF markers *FGF8* and *TBX1*. Together, these data provide evidence that *TBX5*-lineage traced iPSC-CMs exhibit a left ventricular phenotype.

The unexpected finding that our reporter system identified greater than 95% FHF-derived identity raises important questions on whether the standard biphasic WNT protocol used in the generation of hiPSC cardiomyocytes is biased towards the generation of the FHF-lineage. By implementing a lineage tracing method, our reporter system allows for the permanent labeling of descendants from progenitor populations or cardiomyocyte populations that express *TBX5,* which allowed us to evaluate the proportion of definitive ventricular cardiomyocytes that exhibit the FHF phenotype. By having a highly sensitive lineage tracing reporter, we envision this tool can allow for the optimization of differentiation protocols for the generation of SHF derived cell types through the analysis of *TBX5*-lineage negative ventricular cardiomyocytes. Moreover, our results are consistent with an increasing body of literature indicating that current cardiac differentiation protocol appear to bias towards a FHF phenotype as seen in recent cardiac organoid studies showing a high expression level of *HAND1* among generated cardiomyocytes (Drakhlis et al., 2021; Hofbauer et al., 2021). Overall, our reporter system provides a novel tool for the identification of left ventricular-like cardiomyocytes during hiPSC differentiation. By allowing for the permanent labeling of *TBX5* descended cell types, we envision our system being able to conduct more complex studies to study chamber specific cardiomyocyte in the context of congenital

heart diseases as well as other for the generation of novel hiPSC differentiation protocols.

FIGURE LEGENDS

Figure 1: Integration of TBX5-Lineage/MYL2 Reporter System For Isolation of hiPSC-derived Left and Right Ventricular Cardiomyocytes

A) Schematic of standard biphasic WNT modulation protocol for cardiomyocyte differentiation. Bottom schematic indicates overall goal of reporter system for isolation of left and right ventricular cardiomyocytes.

B) Targeting strategy for integration of triple construct system. CMV promoter driven TurboGFP containing a floxed stop cassette and antibiotic resistance gene was targeted to the CCR5 safe harbor site. Dual P2A-Cre construct was targeted to the C-terminus end of the TBX5 gene, and a P2A-TdTomato was targeted to the C-terminus of the MYL2 gene. Red arrows indicate the location of the location of primer pairs used for inside-outside PCR amplification.

C) Inside-Outside PCR data for all three constructs for hiPSC clone containing all three constructs. 5' and 3' bands indicate successful integration of all three constructs. TBX5-Cre construct displays two 5' bands due to 5' end reverse primer binding to Cre recombinase. MYL2 and CCR5 constructs were integrated in a heterozygous manner by the presence of a band amplified using the 5' and 3' outside primers. TBX5-Cre construct was integrated in homozygous manner based on absence of O/O band.

D) Sanger sequencing of MYL2 and TBX5 C-terminus and P2A sequence indicating in-frame integration of the constructs to the 3' end of the genes.

Figure 2: Time Course Analysis of Reporter System Expression Identifies LV Predominant Differentiation

A) Schematic of high-throughput flow cytometric analysis of hiPSC cardiac differentiation using triple reporter system. Cells were collected and fixed at multiple timepoints throughout cardiac development and stained for cardiomyocyte marker cardiac troponin T (TNNT2). Using high throughput flow analyzer, cells were analyzed for GFP, TNNT2, and MYL2-Tomato expression across all timepoints collected.

B) Flow cytometry analysis of TNNT2/TurboGFP expression across hiPSC cardiac differentiation using triple construct reporter line.

C) Quantification of TurboGFP+ cardiomyocytes throughout hiPSC cardiac differentiation. Error bars represent SEM, with individual points representing independent differentiations.

D) Flow cytometry analysis of MYL2-TdTomato/TurboGFP expression for analysis of TBX5-lineage positivity among differentiated ventricular cardiomyocytes.

E) Quantification of TurboGFP+ ventricular cardiomyocytes across day 15, 20, 30 of differentiation. Error bars represent SEM, with individual points representing independent differentiations.

F-G) Representative fluorescent microscopy images of TurboGFP expression and TdTomato expression of day 20 and 30 hiPSC-derived cardiomyocytes.

Figure 3: Gene Expression Analysis of FHF/LV and SHF/RV Markers During hiPSC Cardiac Differentiation

A) RT-qPCR expression of FHF/LV markers *HAND1* and *TBX5* along with expression of *Cre* during hiPSC reporter line differentiation.
B) RT-qPCR expression of known early anterior SHF marker expression *TBX1* and *FGF8.*
C) RT-qPCR expression of pan-cardiac progenitor marker and late stage aSHF marker *ISL1.*
D) RT-qPCR expression of pan-cardiomyocyte marker cardiac troponin-T (TNNT2).
E) RT-qPCR expression of early ventricular cardiomyocyte marker *MYL3* and late-stage ventricular marker *MYL2.*

FIGURE 1

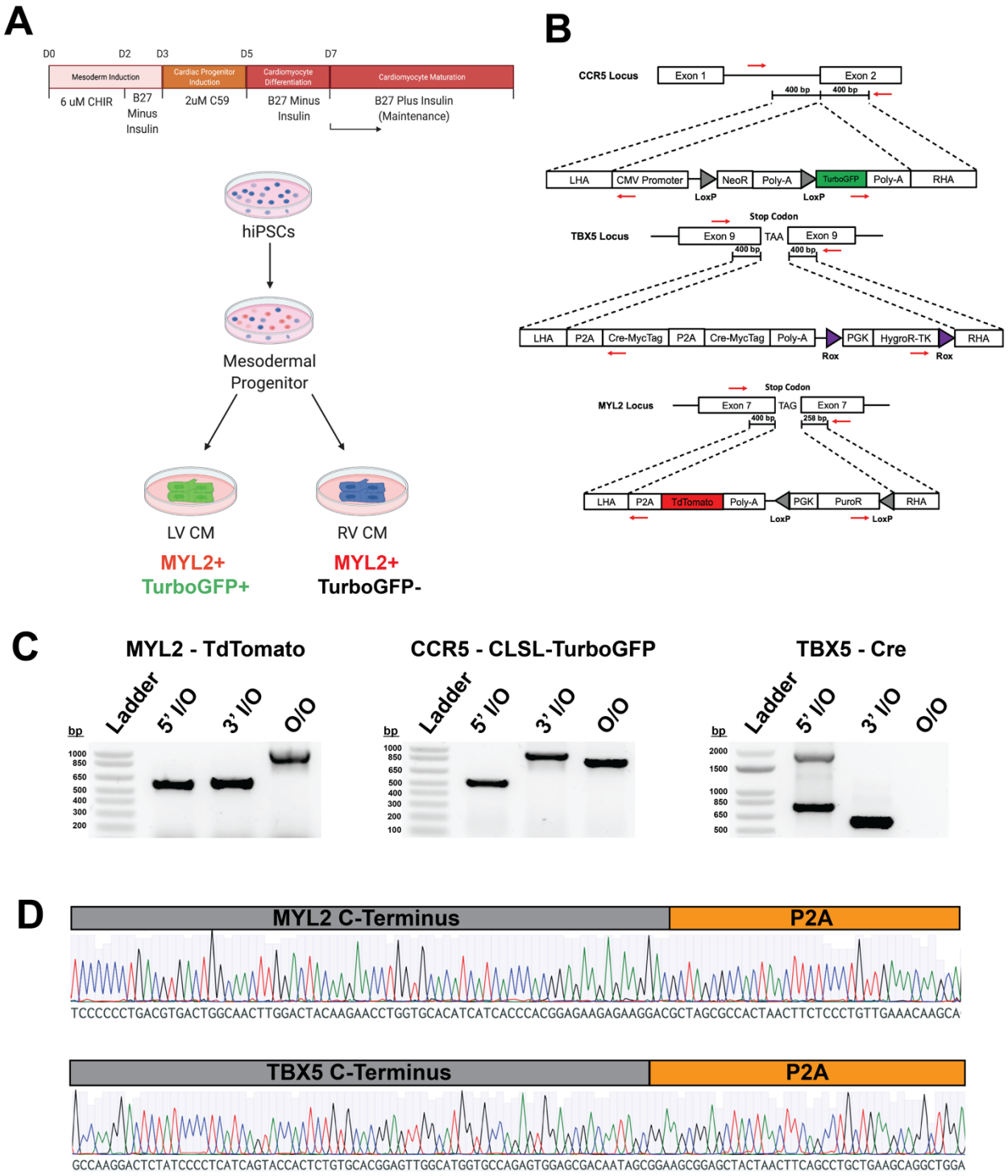
A
D0
D2
D3
D5
D7
Mesoderm Induction
Cardiac Progenitor Induction
Cardiomyocyte Differentiation
Cardiomyocyte Maturation
6 uM CHIR
B27 Minus Insulin
2uM C59
B27 Minus Insulin
B27 Plus Insulin (Maintenance)
hiPSCs
Mesodermal Progenitor
LV CM
MYL2+
TurboGFP+
RV CM
MYL2+
TurboGFP-
B
CCR5 Locus
Exon 1
Exon 2
400 bp
400 bp
LHA
CMV Promoter
NeoR
Poly-A
TurboGFP
Poly-A
RHA
LoxP
LoxP
Stop Codon
TBX5 Locus
Exon 9
TAA
Exon 9
400 bp
400 bp
LHA
P2A
Cre-MycTag
P2A
Cre-MycTag
Poly-A
PGK
HygroR-TK
RHA
Rox
Rox
Stop Codon
MYL2 Locus
Exon 7
TAG
Exon 7
400 bp
258 bp
LHA
P2A
TdTomato
Poly-A
PGK
PuroR
RHA
LoxP
LoxP
C
MYL2 - TdTomato
CCR5 - CLSL-TurboGFP
TBX5 - Cre
bp
Ladder
5' I/O
3' I/O
O/O
1000
850
650
500
400
300
200
100
2000
1500
D
MYL2 C-Terminus
P2A
TCCCCCCTGACGTGACTGGCAACTTGGACTACAAGAACCTGGTGCACATCATCACCCACGGAGAAGAGAAGGACGCTAGCGCCACTAACTTCTCCCTGTTGAAACAAGCA
TBX5 C-Terminus
P2A
GCCAAGGACTCTATCCCCTCATCAGTACCACTCTGTGCACGGAGTTGGCATGGTGCCAGAGTGGAGCGACAATAGCGGAAGCGGAGCTACTAACTTCAGCCTGCTGAAGCAGGCTGGA

FIGURE 2

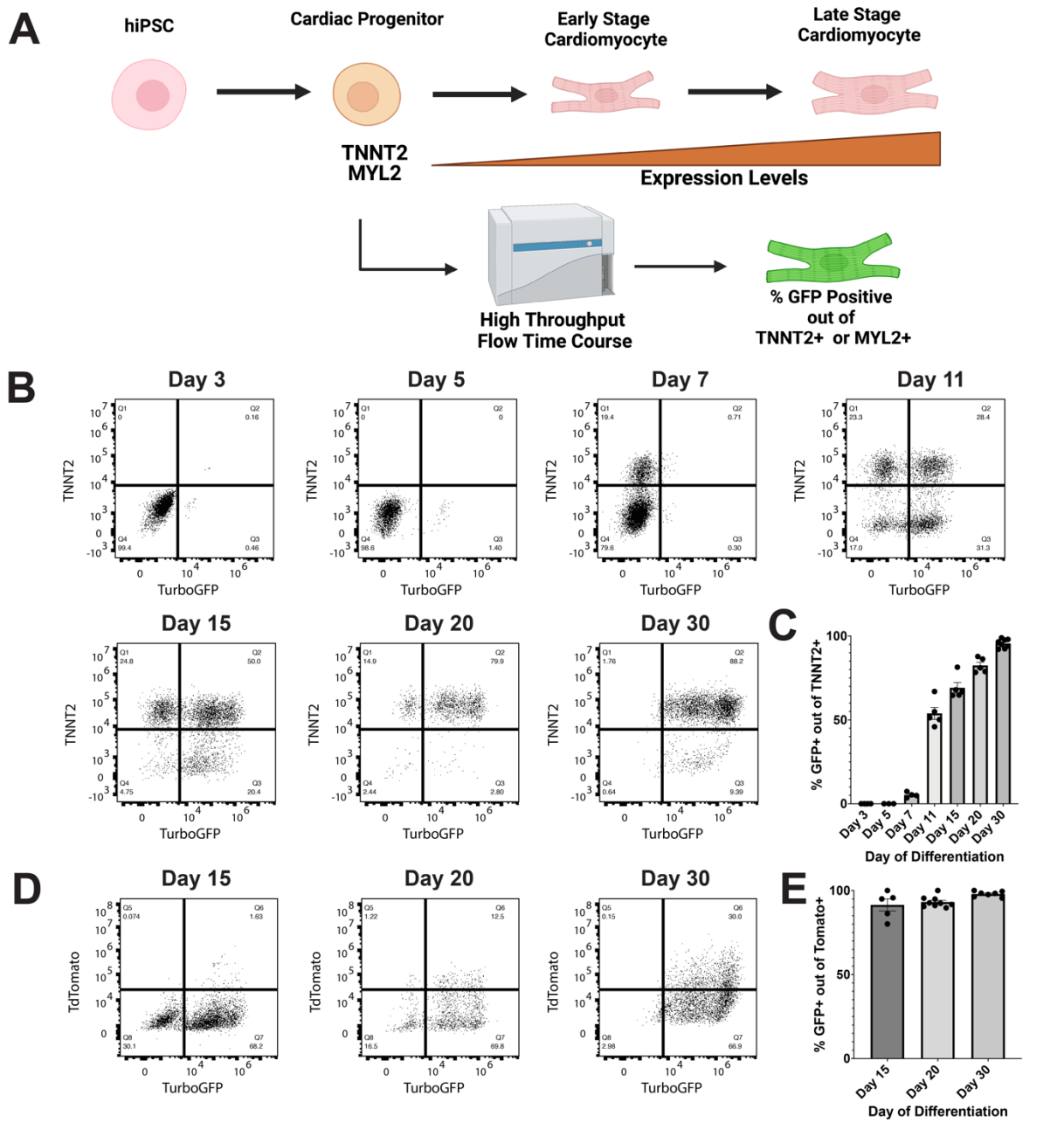
A
hiPSC
Cardiac Progenitor
Early Stage Cardiomyocyte
Late Stage Cardiomyocyte
TNNT2
MYL2
Expression Levels
High Throughput Flow Time Course
% GFP Positive out of TNNT2+ or MYL2+
B
Day 3
Day 5
Day 7
Day 11
Day 15
Day 20
Day 30
TNNT2
TurboGFP
C
% GFP+ out of TNNT2+
Day of Differentiation
D
TdTomato
E
% GFP+ out of Tomato+
F
Day 20
G
Day 30
TurboGFP
TdTomato
200 µm

FIGURE 3

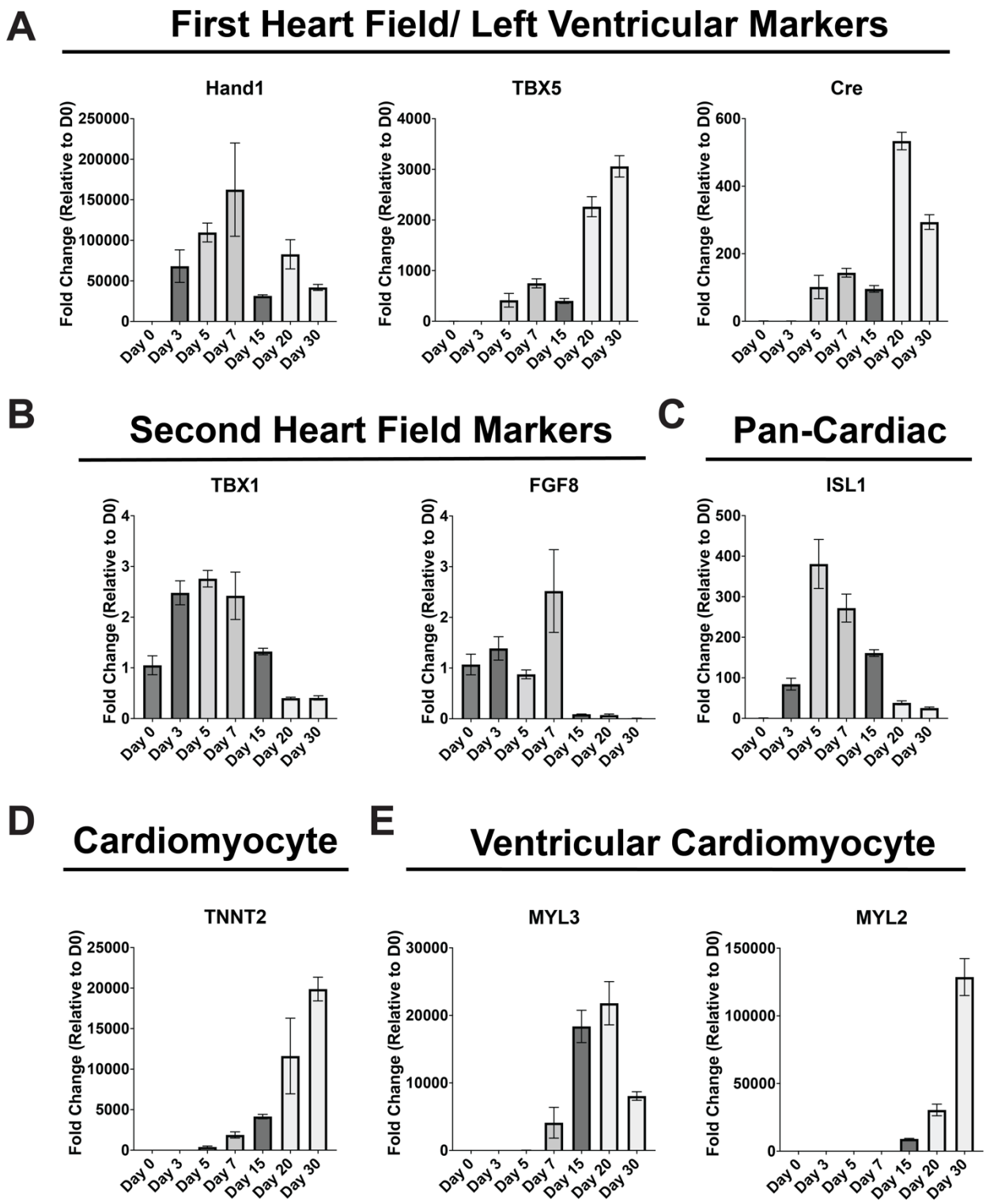
A
First Heart Field/ Left Ventricular Markers
Hand1
TBX5
Cre
B
Second Heart Field Markers
TBX1
FGF8
C
Pan-Cardiac
ISL1
D
Cardiomyocyte
TNNT2
E
Ventricular Cardiomyocyte
MYL3
MYL2
Fold Change (Relative to D0)
Day 0
Day 3
Day 5
Day 7
Day 15
Day 20
Day 30

REFERENCES

Asp, M., Giacomello, S., Larsson, L., Wu, C., Fürth, D., Qian, X., Wärdell, E., Custodio, J., Reimegård, J., Salmén, F., Österholm, C., Ståhl, P.L., Sundström, E., Åkesson, E., Bergmann, O., Bienko, M., Månsson-Broberg, A., Nilsson, M., Sylvén, C., Lundeberg, J., 2019. A Spatiotemporal Organ-Wide Gene Expression and Cell Atlas of the Developing Human Heart. Cell 179, 1647-1660.e19. https://doi.org/10.1016/j.cell.2019.11.025

Barnes, R.M., Firulli, B.A., Conway, S.J., Vincentz, J.W., Firulli, A.B., 2010. Analysis of the Hand1 Cell Lineage Reveals Novel Contributions to Cardiovascular, Neural Crest, Extra-Embryonic, and Lateral Mesoderm Derivatives. Dev Dyn 239, 3086–3097. https://doi.org/10.1002/dvdy.22428

Bruneau, B.G., Logan, M., Davis, N., Levi, T., Tabin, C.J., Seidman, J.G., Seidman, C.E., 1999. Chamber-specific cardiac expression of Tbx5 and heart defects in Holt-Oram syndrome. Dev Biol 211, 100–108. https://doi.org/10.1006/dbio.1999.9298

Bruneau, B.G., Nemer, G., Schmitt, J.P., Charron, F., Robitaille, L., Caron, S., Conner, D.A., Gessler, M., Nemer, M., Seidman, C.E., Seidman, J.G., 2001. A Murine Model of Holt-Oram Syndrome Defines Roles of the T-Box Transcription Factor Tbx5 in Cardiogenesis and Disease. Cell 106, 709–721. https://doi.org/10.1016/S0092-8674(01)00493-7

Buijtendijk, M.F.J., Barnett, P., Hoff, M.J.B. van den, 2020. Development of the human heart. American Journal of Medical Genetics Part C: Seminars in Medical Genetics 184, 7–22. https://doi.org/10.1002/ajmg.c.31778

Burridge, P.W., Holmström, A., Wu, J.C., 2015. Chemically Defined Culture and Cardiomyocyte Differentiation of Human Pluripotent Stem Cells. Curr Protoc Hum Genet 87, 21.3.1-21.3.15. https://doi.org/10.1002/0471142905.hg2103s87

Cai, C.-L., Liang, X., Shi, Y., Chu, P.-H., Pfaff, S.L., Chen, J., Evans, S., 2003. Isl1 identifies a cardiac progenitor population that proliferates prior to differentiation and contributes a majority of cells to the heart. Dev Cell 5, 877–889. https://doi.org/10.1016/s1534-5807(03)00363-0

Cavaliere, G., 2017. A 14-day limit for bioethics: the debate over human embryo research. BMC Medical Ethics 18, 38. https://doi.org/10.1186/s12910-017-0198-5

Chen, I.Y., Matsa, E., Wu, J.C., 2016. Induced Pluripotent Stem Cells: at the Heart of Cardiovascular Precision Medicine. Nat Rev Cardiol 13, 333–349. https://doi.org/10.1038/nrcardio.2016.36

Chirikian, O., Goodyer, W.R., Dzilic, E., Serpooshan, V., Buikema, J.W., McKeithan, W., Wu, H., Li, G., Lee, S., Merk, M., Galdos, F., Beck, A., Ribeiro, A.J.S., Paige, S., Mercola, M., Wu, J.C., Pruitt, B.L., Wu, S.M., 2021. CRISPR/Cas9-based targeting of fluorescent reporters to human iPSCs to isolate atrial and ventricular-specific cardiomyocytes. Sci Rep 11, 3026. https://doi.org/10.1038/s41598-021-81860-x

Cui, Y., Zheng, Y., Liu, X., Yan, L., Fan, X., Yong, J., Hu, Y., Dong, J., Li, Q., Wu, X., Gao, S., Li, J., Wen, L., Qiao, J., Tang, F., 2019. Single-Cell Transcriptome

Analysis Maps the Developmental Track of the Human Heart. Cell Rep 26, 1934-1950.e5. https://doi.org/10.1016/j.celrep.2019.01.079
de Soysa, T.Y., Ranade, S.S., Okawa, S., Ravichandran, S., Huang, Y., Salunga, H.T., Schricker, A., del Sol, A., Gifford, C.A., Srivastava, D., 2019. Single-cell analysis of cardiogenesis reveals basis for organ-level developmental defects. Nature 572, 120–124. https://doi.org/10.1038/s41586-019-1414-x
DeLaughter, D.M., Bick, A.G., Wakimoto, H., McKean, D., Gorham, J.M., Kathiriya, I.S., Hinson, J.T., Homsy, J., Gray, J., Pu, W., Bruneau, B.G., Seidman, J.G., Seidman, C.E., 2016. Single-Cell Resolution of Temporal Gene Expression during Heart Development. Developmental Cell 39, 480–490. https://doi.org/10.1016/j.devcel.2016.10.001
Devine, W.P., Wythe, J.D., George, M., Koshiba-Takeuchi, K., Bruneau, B.G., 2014. Early patterning and specification of cardiac progenitors in gastrulating mesoderm. eLife 3, e03848. https://doi.org/10.7554/eLife.03848
Devine, W.P., Wythe, J.D., George, M., Koshiba-Takeuchi, K., Bruneau, B.G., n.d. Early patterning and specification of cardiac progenitors in gastrulating mesoderm. eLife 3, e03848. https://doi.org/10.7554/eLife.03848
Drakhlis, L., Biswanath, S., Farr, C.-M., Lupanow, V., Teske, J., Ritzenhoff, K., Franke, A., Manstein, F., Bolesani, E., Kempf, H., Liebscher, S., Schenke-Layland, K., Hegermann, J., Nolte, L., Meyer, H., de la Roche, J., Thiemann, S., Wahl-Schott, C., Martin, U., Zweigerdt, R., 2021. Human heart-forming organoids recapitulate early heart and foregut development. Nat Biotechnol 39, 737–746. https://doi.org/10.1038/s41587-021-00815-9
Feyen, D.A.M., McKeithan, W.L., Bruyneel, A.A.N., Spiering, S., Hörmann, L., Ulmer, B., Zhang, H., Briganti, F., Schweizer, M., Hegyi, B., Liao, Z., Pölönen, R.-P., Ginsburg, K.S., Lam, C.K., Serrano, R., Wahlquist, C., Kreymerman, A., Vu, M., Amatya, P.L., Behrens, C.S., Ranjbarvaziri, S., Maas, R.G.C., Greenhaw, M., Bernstein, D., Wu, J.C., Bers, D.M., Eschenhagen, T., Metallo, C.M., Mercola, M., 2020. Metabolic Maturation Media Improve Physiological Function of Human iPSC-Derived Cardiomyocytes. Cell Rep 32, 107925. https://doi.org/10.1016/j.celrep.2020.107925
Galdos, F.X., Darsha, A.K., Paige, S.L., Wu, S.M., 2021. Purification of Pluripotent Stem Cell-Derived Cardiomyocytes Using CRISPR/Cas9-Mediated Integration of Fluorescent Reporters. Methods Mol Biol 2158, 223–240. https://doi.org/10.1007/978-1-0716-0668-1_17
Hofbauer, P., Jahnel, S.M., Papai, N., Giesshammer, M., Deyett, A., Schmidt, C., Penc, M., Tavernini, K., Grdseloff, N., Meledeth, C., Ginistrelli, L.C., Ctortecka, C., Šalic, Š., Novatchkova, M., Mendjan, S., 2021. Cardioids reveal self-organizing principles of human cardiogenesis. Cell 184, 3299-3317.e22. https://doi.org/10.1016/j.cell.2021.04.034
Hrstka, S.C.L., Li, X., Nelson, T.J., 2017. NOTCH1-Dependent Nitric Oxide Signaling Deficiency in Hypoplastic Left Heart Syndrome Revealed Through Patient-Specific Phenotypes Detected in Bioengineered Cardiogenesis. STEM CELLS 35, 1106–1119. https://doi.org/10.1002/stem.2582
Lahm, H., Jia, M., Dreßen, M., Wirth, F., Puluca, N., Gilsbach, R., Keavney, B.D., Cleuziou, J., Beck, N., Bondareva, O., Dzilic, E., Burri, M., König, K.C.,

Ziegelmüller, J.A., Abou-Ajram, C., Neb, I., Zhang, Z., Doppler, S.A., Mastantuono, E., Lichtner, P., Eckstein, G., Hörer, J., Ewert, P., Priest, J.R., Hein, L., Lange, R., Meitinger, T., Cordell, H.J., Müller-Myhsok, B., Krane, M., 2021. Congenital heart disease risk loci identified by genome-wide association study in European patients. J Clin Invest 131. https://doi.org/10.1172/JCI141837

Lee, J.H., Protze, S.I., Laksman, Z., Backx, P.H., Keller, G.M., 2017. Human Pluripotent Stem Cell-Derived Atrial and Ventricular Cardiomyocytes Develop from Distinct Mesoderm Populations. Cell Stem Cell 21, 179-194.e4. https://doi.org/10.1016/j.stem.2017.07.003

Li, G., Xu, A., Sim, S., Priest, J.R., Tian, X., Khan, T., Quertermous, T., Zhou, B., Tsao, P.S., Quake, S.R., Wu, S.M., 2016. Transcriptomic Profiling Maps Anatomically Patterned Subpopulations among Single Embryonic Cardiac Cells. Developmental Cell 39, 491–507. https://doi.org/10.1016/j.devcel.2016.10.014

Lian, X., Zhang, J., Azarin, S.M., Zhu, K., Hazeltine, L.B., Bao, X., Hsiao, C., Kamp, T.J., Palecek, S.P., 2013. Directed cardiomyocyte differentiation from human pluripotent stem cells by modulating Wnt/β-catenin signaling under fully defined conditions. Nat Protoc 8, 162–175. https://doi.org/10.1038/nprot.2012.150

Liu, Z., Chen, O., Wall, J.B.J., Zheng, M., Zhou, Y., Wang, L., Ruth Vaseghi, H., Qian, L., Liu, J., 2017. Systematic comparison of 2A peptides for cloning multi-genes in a polycistronic vector. Sci Rep 7, 2193. https://doi.org/10.1038/s41598-017-02460-2

Ma, Q., Zhou, B., Pu, W.T., 2008. Reassessment of Isl1 and Nkx2-5 cardiac fate maps using a Gata4-based reporter of Cre activity. Dev Biol 323, 98–104. https://doi.org/10.1016/j.ydbio.2008.08.013

Matsuda, T., Cepko, C.L., 2007. Controlled expression of transgenes introduced by in vivo electroporation. Proc Natl Acad Sci U S A 104, 1027–1032. https://doi.org/10.1073/pnas.0610155104

Meilhac, S.M., Buckingham, M.E., 2018. The deployment of cell lineages that form the mammalian heart. Nat Rev Cardiol 15, 705–724. https://doi.org/10.1038/s41569-018-0086-9

Meilhac, S.M., Esner, M., Kelly, R.G., Nicolas, J.-F., Buckingham, M.E., 2004. The clonal origin of myocardial cells in different regions of the embryonic mouse heart. Dev Cell 6, 685–698. https://doi.org/10.1016/s1534-5807(04)00133-9

Miao, Y., Tian, L., Martin, M., Paige, S.L., Galdos, F.X., Li, J., Klein, A., Zhang, H., Ma, N., Wei, Y., Stewart, M., Lee, S., Moonen, J.-R., Zhang, B., Grossfeld, P., Mital, S., Chitayat, D., Wu, J.C., Rabinovitch, M., Nelson, T.J., Nie, S., Wu, S.M., Gu, M., 2020. Intrinsic Endocardial Defects Contribute to Hypoplastic Left Heart Syndrome. Cell Stem Cell 27, 574-589.e8. https://doi.org/10.1016/j.stem.2020.07.015

Paige, S.L., Galdos, F.X., Lee, S., Chin, E.T., Ranjbarvaziri, S., Feyen, D.A.M., Darsha, A.K., Xu, S., Ryan, J.A., Beck, A.L., Qureshi, M.Y., Miao, Y., Gu, M., Bernstein, D., Nelson, T.J., Mercola, M., Rabinovitch, M., Ashley, E.A., Parikh, V.N., Wu, S.M., 2020. Patient-Specific Induced Pluripotent Stem Cells Implicate Intrinsic Impaired Contractility in Hypoplastic Left Heart Syndrome. Circulation 142, 1605–1608. https://doi.org/10.1161/CIRCULATIONAHA.119.045317

Park, E.J., Watanabe, Y., Smyth, G., Miyagawa-Tomita, S., Meyers, E., Klingensmith, J., Camenisch, T., Buckingham, M., Moon, A.M., 2008. An FGF autocrine loop initiated in second heart field mesoderm regulates morphogenesis at the arterial pole of the heart. Development 135, 3599–3610. https://doi.org/10.1242/dev.025437

Protze, S.I., Liu, J., Nussinovitch, U., Ohana, L., Backx, P.H., Gepstein, L., Keller, G.M., 2017. Sinoatrial node cardiomyocytes derived from human pluripotent cells function as a biological pacemaker. Nat Biotechnol 35, 56–68. https://doi.org/10.1038/nbt.3745

Rana, M.S., Théveniau-Ruissy, M., De Bono, C., Mesbah, K., Francou, A., Rammah, M., Domínguez, J.N., Roux, M., Laforest, B., Anderson, R.H., Mohun, T., Zaffran, S., Christoffels, V.M., Kelly, R.G., 2014. Tbx1 coordinates addition of posterior second heart field progenitor cells to the arterial and venous poles of the heart. Circ Res 115, 790–799. https://doi.org/10.1161/CIRCRESAHA.115.305020

Reller, M.D., Strickland, M.J., Riehle-Colarusso, T., Mahle, W.T., Correa, A., 2008. Prevalence of Congenital Heart Defects in Metropolitan Atlanta, 1998-2005. The Journal of Pediatrics 153, 807–813. https://doi.org/10.1016/j.jpeds.2008.05.059

Rhee, S., Paik, D.T., Yang, J.Y., Nagelberg, D., Williams, I., Tian, L., Roth, R., Chandy, M., Ban, J., Belbachir, N., Kim, S., Zhang, H., Phansalkar, R., Wong, K.M., King, D.A., Valdez, C., Winn, V.D., Morrison, A.J., Wu, J.C., Red-Horse, K., 2021. Endocardial/endothelial angiocrines regulate cardiomyocyte development and maturation and induce features of ventricular non-compaction. Eur Heart J ehab298. https://doi.org/10.1093/eurheartj/ehab298

Rowe, R.G., Daley, G.Q., 2019. Induced pluripotent stem cells in disease modelling and drug discovery. Nat Rev Genet 20, 377–388. https://doi.org/10.1038/s41576-019-0100-z

Sacchetto, C., Vitiello, L., de Windt, L.J., Rampazzo, A., Calore, M., 2020. Modeling Cardiovascular Diseases with hiPSC-Derived Cardiomyocytes in 2D and 3D Cultures. Int J Mol Sci 21, 3404. https://doi.org/10.3390/ijms21093404

Yang, C., Xu, Y., Yu, M., Lee, D., Alharti, S., Hellen, N., Ahmad Shaik, N., Banaganapalli, B., Sheikh Ali Mohamoud, H., Elango, R., Przyborski, S., Tenin, G., Williams, S., O'Sullivan, J., Al-Radi, O.O., Atta, J., Harding, S.E., Keavney, B., Lako, M., Armstrong, L., 2017. Induced pluripotent stem cell modelling of HLHS underlines the contribution of dysfunctional NOTCH signalling to impaired cardiogenesis. Human Molecular Genetics 26, 3031–3045. https://doi.org/10.1093/hmg/ddx140

Zaffran, S., Kelly, R.G., Meilhac, S.M., Buckingham, M.E., Brown, N.A., 2004. Right ventricular myocardium derives from the anterior heart field. Circ Res 95, 261–268. https://doi.org/10.1161/01.RES.0000136815.73623.BE